Pictorial essay

Cite as: Alyanak B, Dede BT, Bağcıer F, Yıldızgören MT: Ultrasound of the common peroneal nerve at the knee: a structured scanning protocol. J Ultrason 2026; 26: 8. doi: 10.15557/JoU.2026.0008.

Submitted: 07.01.2026
Accepted: 09.02.2026
Published: 31.03.2026

Ultrasound of the common peroneal nerve at the knee: a structured scanning protocol

Bülent Alyanak[1], Burak Tayyip Dede[2], Fatih Bağcıer[3], Mustafa Turgut Yıldızgören[4]

[1] *Department of Physical Medicine and Rehabilitation, Gölcük Necati Çelik State Hospital, Turkey*
[2] *Department of Physical Medicine and Rehabilitation, Prof. Dr. Cemil Taşçıoğlu City Hospital, Turkey*
[3] *Department of Physical Medicine and Rehabilitation, Başakşehir Çam and Sakura City Hospital, Turkey*
[4] *Department of Physical Medicine and Rehabilitation, Necmettin Erbakan University, Faculty of Medicine, Turkey*

Corresponding author: Bülent Alyanak; e-mail: bulentalyanak@hotmail.com

DOI: 10.15557/JoU.2026.0008

Keywords
common peroneal nerve; peripheral nerve ultrasound; peroneal neuropathy; fibular head; peroneal tunnel

Abstract

The common peroneal nerve is one of the most frequent sites of neuropathy around the knee. Owing to its superficial course, it is highly vulnerable to both trauma and mechanical compression. High-frequency ultrasonography enables real-time, dynamic evaluation of the common peroneal nerve along its entire trajectory from the popliteal fossa to the exit from the peroneal tunnel. This article presents a stepwise, structured ultrasound protocol for the assessment of the common peroneal nerve in the peri-knee region. Supported by illustrative images and videos, the protocol is expected to facilitate practical applicability in daily practice and improve diagnostic accuracy. Furthermore, the guiding role of ultrasonography in interventional planning is highlighted.

Introduction

The common peroneal nerve (CPN) branches from the sciatic nerve within the popliteal fossa and then courses into the lateral compartment, becoming superficial around the fibular head and neck before dividing into its terminal branches within the peroneal tunnel. The peroneal tunnel is the fibro-muscular/osteo-fibrous passage at the fibular neck through which the CPN travels; the neck of the fibula forms the floor of the tunnel, while the entrance is created by a musculo-aponeurotic arch derived from the soleus and peroneus longus muscles[(1)]. This anatomical pathway renders the nerve particularly susceptible to both superficial trauma and mechanical compression. Consequently, the fibular head and peroneal tunnel have been identified as the most frequent sites of peroneal neuropathies[(2,3)]. Clinical manifestations may include pain, foot drop, gait disturbance, and a marked decline in quality of life.

Although electrophysiology remains the gold standard for diagnosis, it provides only functional information and often fails to identify the underlying anatomical causes. In recent years, high-resolution ultrasonography (US) has become indispensable for the direct assessment of peripheral nerves and the detection of associated structural etiologies. US not only demonstrates nerve caliber and fascicular architecture, but also delineates concomitant cystic or tumoral lesions, post-traumatic alterations, and anatomical variants[(2,4–6)]. In addition, US-guided interventional procedures play an important role in therapeutic planning[(7,8)].

Although CSA values and diagnostic thresholds have been described in the literature, a structured, stepwise US protocol for assessing the course of the CPN around the knee has not previously been reported. This study aims to present a stepwise, structured US examination protocol for the CPN, based on its normal anatomical and topographic course from the popliteal fossa to the exit from the peroneal tunnel, and to define reproducible reference points and imaging landmarks at each level.

US scanning protocol

Equipment and settings

For the evaluation of nerves around the knee, a high-frequency linear transducer (12–18 MHz) should be used. To optimize image quality, a nerve preset providing high spatial resolution is recommended, and the focus and gain should be adjusted until the epineurial contours are sharply delineated.

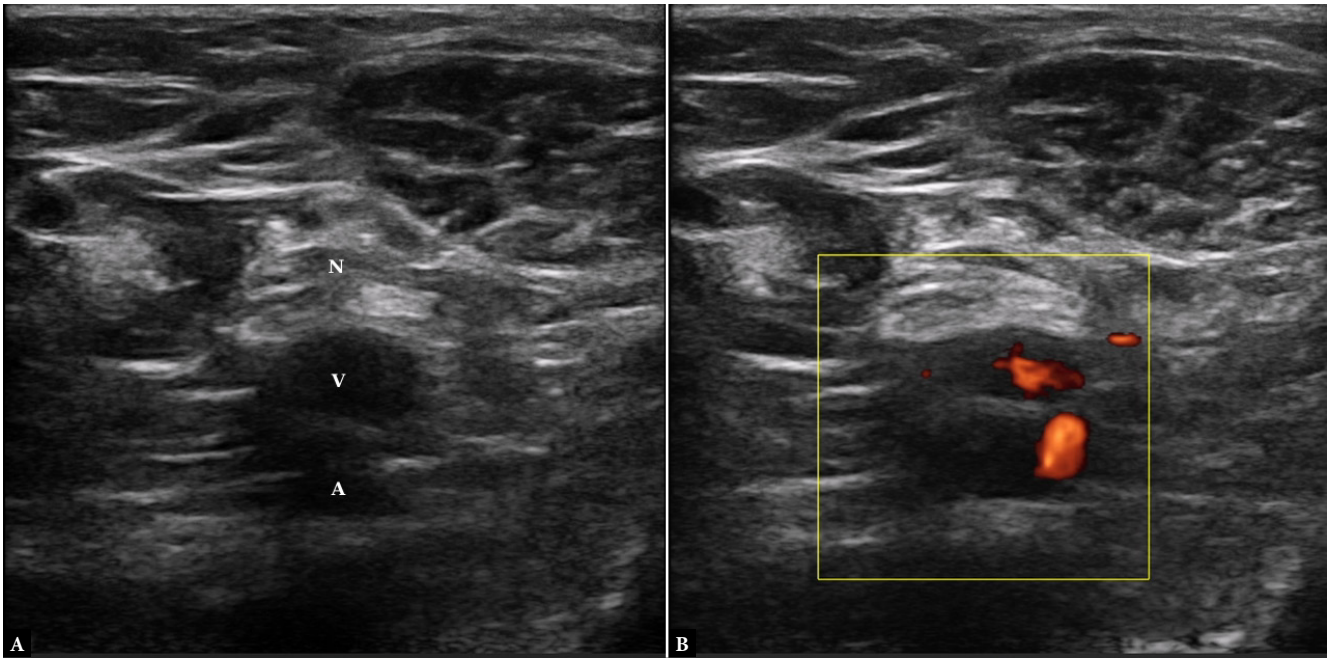

Fig. 1. *Short-axis ultrasound images of the right popliteal fossa.* **A.** *Gray-scale image demonstrating the typical topographic relationship between the sciatic nerve and adjacent vascular structures.* **B.** *Power Doppler image at the same level, facilitating differentiation of the artery and vein and confirming the position of the nerve relative to the vessels. N – nerve; A – artery; V – vein*

Patient positioning

The optimal position is prone, with the knee slightly flexed, which promotes muscle relaxation and facilitates nerve visualization. Alternatively, lateral decubitus or supine positions may be used, particularly during interventional planning.

Step 1. Proximal to the popliteal fossa (distal posterior thigh)

Scanning should be initiated in the short axis proximal to the popliteal fossa, at the level of the distal posterior thigh. At this level, the popliteal artery is typically the deepest structure, with the popliteal vein superficial to it, and the sciatic nerve occupying the most superficial–lateral position (Fig. 1). Because the vein may collapse with transducer pressure or muscle contraction, its relationship to the artery should serve as the primary reference. The sciatic nerve is readily identified by its ovoid contour and hypoechoic fascicular pattern. When traced from proximal to distal, its consistent topographic relationship with the artery and vein enables reliable tracking. Given the variable level of sciatic division, the nerve may appear as a single trunk at this site, or as a "dual-component" configuration in which the tibial and common peroneal components course in close proximity within a shared sheath. After confirming the sciatic trunk, the nerve should be followed distally. On entering the popliteal fossa (at its superior end), the topographic separation of the tibial nerve and the CPN can be demonstrated in the short axis (Fig. 2). Power Doppler facilitates confirmation of the arterial–venous distinction, reinforces orientation based on the vascular bundle, and supports accurate localization of the neural structures. This approach standardizes the starting point at the pre-division sciatic trunk while enabling reliable identification of the tibial and common peroneal nerves during distal tracking.

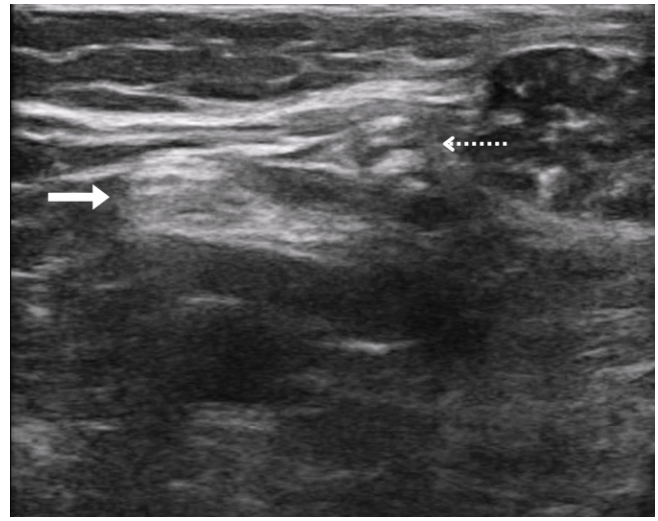

Fig. 2. *Short-axis ultrasound image at the level of the sciatic nerve bifurcation, demonstrating division into the tibial nerve and the common peroneal nerve. The solid white arrow indicates the tibial nerve, and the dashed white arrow indicates the common peroneal nerve*

Step 2. Lateral femoral condyle level

With continued distal advancement in the short axis, the CPN courses superficially between the biceps femoris and the lateral head of the gastrocnemius muscle (Fig. 3). At this level, the nerve is easily

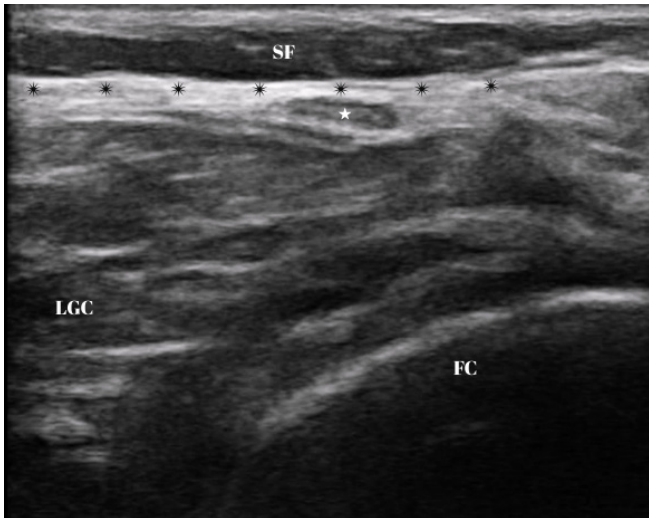

Fig. 3. *Short-axis ultrasound image at the level of the lateral femoral condyle. The white star marks the common peroneal nerve, and the black asterisk marks the crural fascia. SF – subcutaneous fat; FC – femoral condyle; LGC – lateral head of the gastrocnemius muscle*

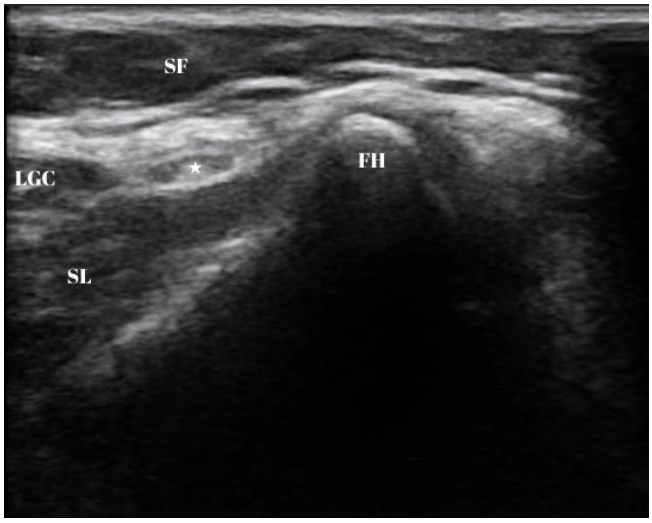

Fig. 4. *Short-axis ultrasound image at the level of the fibular head. The white star marks the common peroneal nerve. LGC – lateral head of the gastrocnemius muscle; FH – fibular head; SL – soleus muscle; SF – subcutaneous fat*

visualized due to its subcutaneous location and can be recognized by its ovoid fascicular appearance. However, anisotropy artifact is common, and fine probe adjustments are critical to maintain the true echogenicity of the nerve. Clear demonstration of the surrounding muscle planes aids in confirming the topographic position and provides a reliable landmark for tracking the nerve distally.

Step 3. Fibular head/neck

At the fibular head, the CPN lies very close to the bone, and the fibular apex typically serves as a prominent landmark (Fig. 4). As the probe is advanced distally toward the fibular neck, the apex disappears and the nerve appears flatter in the short axis (Fig. 5). Documenting both the head and neck levels separately is essential for accurate identification of anatomical references, making this transition one of the critical steps in the protocol. In this study, the "fibular head" refers specifically to the apex capitis fibula, the sharp projection articulating with the tibia, whereas the "fibular neck" denotes the immediately distal, flattened segment. In the literature, the term "fibular head" is sometimes used more broadly to encompass both regions; however, in our protocol, the two structures are distinctly and explicitly differentiated[9].

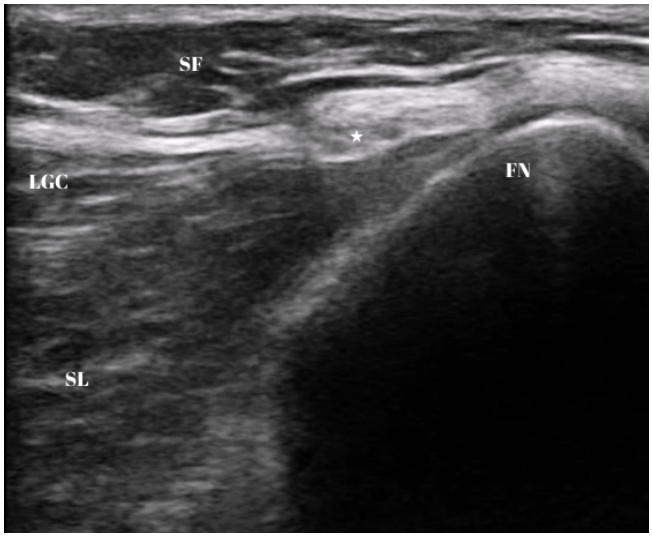

Fig. 5. *Short-axis ultrasound image at the level of the fibular neck. The white star marks the common peroneal nerve. LGC – lateral head of the gastrocnemius muscle; FN – fibular neck; SL – soleus muscle; SF – subcutaneous fat*

Step 4. Peroneal tunnel

Beyond the fibular neck, the CPN passes beneath the peroneus longus muscle and continues within the peroneal tunnel (Fig. 6). At this level, the nerve appears in the short axis as a hyperechoic fascicular structure coursing between muscle fibers. When followed distally, the bifurcation of the nerve into its superficial (SPN) and deep (DPN) branches can be visualized (Fig. 7). The superficial branch courses laterally toward the subcutaneous tissue, whereas the deep branch traverses into the anterior compartment, accompanying the tibialis anterior artery. Documentation of this branching point is crucial for anatomical standardization and for the recognition of potential variations.

The complete stepwise scanning protocol, from the popliteal fossa through the sequential course of the CPN to its bifurcation into the superficial and deep branches, is demonstrated in Video 1 and Video 2.

Recurrent articular branch

The recurrent articular branch of the CPN extends toward the proximal tibiofibular joint and plays a pivotal role in the pathogenesis of intraneural ganglion cysts, as postulated in the "articular theory"[10]. Although the clinical significance of this branch in surgical planning is well recognized, to the best of our knowledge,

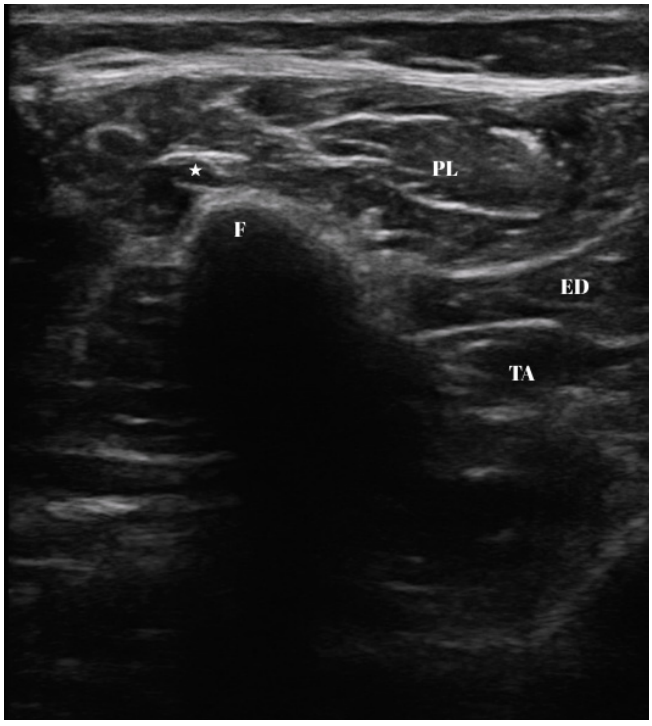

Fig. 6. *Short-axis ultrasound image at the entrance of the peroneal tunnel. The white star marks the common peroneal nerve. PL – peroneus longus muscle; ED – extensor digitorum muscle; TA – tibialis anterior muscle; F – fibula*

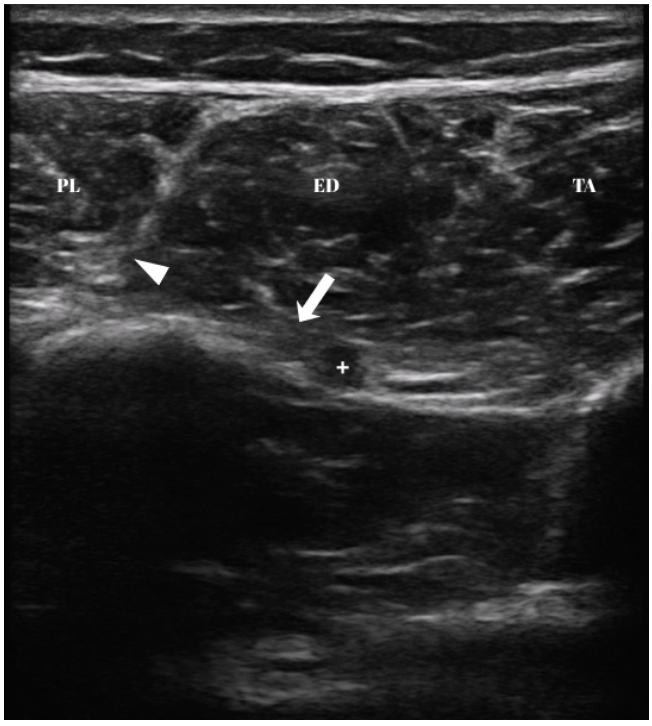

Fig. 7. *Short-axis ultrasound image at the distal peroneal tunnel. The white arrowhead indicates the superficial peroneal nerve, the white arrow indicates the deep peroneal nerve, and the plus sign (+) marks the tibial artery. PL – peroneus longus muscle; ED – extensor digitorum muscle; TA – tibialis anterior muscle*

no published case series or technical report has demonstrated clear and reliable visualization using high-frequency US. Consistent with the current literature, this branch could not be reliably identified on US in our study. This represents one of the limitations of our work.

Standard measurements and threshold values

The most reliable levels for caliber assessment of the CPN are the popliteal fossa and the fibular head/neck. Measurements should be obtained in the short-axis plane using manual planimetry along the inner border of the epineurium, while maintaining minimal probe compression. In healthy adults, reference values reported in a multicenter meta-analysis by Fisse et al.[4] were 8.4 mm² (95% CI: 6.8–9.9) at the fibular head and 7.9 mm² (95% CI: 6.6–9.2) at the popliteal fossa. Because no significant side-to-side differences have been reported, contralateral comparison is considered a reliable internal reference.

Kim et al.[11] demonstrated that in patients with electrophysiologically confirmed peroneal neuropathy, a fibular-head CSA greater than 11.7 mm² yielded 85% sensitivity and 90% specificity, while a side-to-side CSA difference of ≥1.7 mm² increased specificity to 96.7%. In addition, a fibular head-to-popliteal fossa CSA ratio greater than 1.11 was found to be significant for pathology, and a symptomatic-to-asymptomatic side ratio greater than 1.24 provided 72.2% sensitivity and 96.7% specificity. For this reason, absolute CSA, contralateral differences, and ratio-based assessments should be used in combination.

Recent studies have demonstrated that ultrasonographic measurements strongly complement electrophysiology. In particular, a significant correlation has been observed between the side-to-side CSA ratio (STS ratio) and compound muscle action potential (CMAP) amplitude. An abnormal STS ratio increased the likelihood of an abnormal CMAP by nearly 18-fold, and each unit increase in the STS ratio was associated with an average decrease of 2.8 mV in CMAP amplitude[5].

During the stepwise assessment, the operator should also screen for common pathologic causes of CPN compromise around the fibular tunnel, including ganglion or synovial cysts (often arising from the proximal tibiofibular joint), post-traumatic hematoma or scar tissue, and other space-occupying lesions. These conditions may be associated with focal nerve enlargement, altered echotexture, loss of fascicular definition, and/or direct mass effect. Careful evaluation of their relationship to the nerve can aid diagnosis and guide management.

US is a strong first-line imaging modality for CPN neuropathy[12], and in recent years studies have begun to show that it is superior to MRI. For example, in the study published by Oosterbos et al.[6] in 2024, it was reported that US reliably demonstrated CSA enlargement, echotexture changes, and relationships with adjacent structures, whereas MRI was superior for detecting intraneural signal abnormalities and muscle-denervation findings. In a 2025 study by Tagliero et al.[13], US showed high sensitivity and specificity in the diagnosis of CPN lesions and provided more accurate results than MRI.

Although CSA reference values and diagnostic thresholds have been described in the literature, to the best of our knowledge, few publications have comprehensively outlined the course of the CPN from the popliteal fossa to the exit of the peroneal tunnel using a stepwise scanning approach with practical reference points and imaging landmarks at each level. This study systematically summarizes the nerve's normal anatomical and topographic features, and proposes a practical, readily implementable, and reproducible US scanning workflow for clinical use. However, formal assessment of measurement reproducibility (intra- and inter-observer reliability) was not performed. This structured protocol may support standardization in daily practice and facilitate interventional planning, thereby providing a practical framework for clinicians.

Conflict of interest

The authors do not report any financial or personal connections with other persons or organizations which might negatively affect the contents of this publication and/or claim authorship rights to this publication.

Author contributions

Original concept of study: BA, FB. Writing of manuscript: BA. Analysis and interpretation of data: BA, BTD. Final acceptation of manuscript: BA, BTD, MTY. Collection, recording and/or compilation of data: BA, BTD, FB, MTY. Critical review of manuscript: BA, BTD, FB, MTY.

References

1. Ryan W, Mahony N, Delaney M, O'Brien M, Murray P. Relationship of the common peroneal nerve and its branches to the head and neck of the fibula. Clin Anat. 2003 Nov;16(6):501–505. doi: 10.1002/ca.10155.
2. Kumar S, Mangi MD, Zadow S, Lim W. Nerve entrapment syndromes of the lower limb: a pictorial review. Insights Imaging. 2023 Oct 2;14(1):166. doi: 10.1186/s13244-023-01514-6.
3. Donovan A, Rosenberg ZS, Cavalcanti CF. MR imaging of entrapment neuropathies of the lower extremity. Part 2. The knee, leg, ankle, and foot. Radiographics. 2010 Jul-Aug;30(4):1001–1019. doi: 10.1148/rg.304095188.
4. Fisse AL, Katsanos AH, Gold R, Krogias C, Pitarokoili K. Cross-sectional area reference values for peripheral nerve ultrasound in adults: A systematic review and meta-analysis-Part II: Lower extremity nerves. Eur J Neurol. 2021 Jul;28(7):2313–2318. doi: 10.1111/ene.14850.
5. DeMartini SJ, Faust AM, Olafsen NP, Brogan DM, Dy CJ. Ultrasound as a complementary tool to electrodiagnostics in the evaluation of compressive neuropathy of the common fibular nerve. HSS J. 2025 May;21(2):146–151. doi: 10.1177/15563316241285898.
6. Oosterbos C, Weerdt O, Lembrechts M, Radwan A, Brys P, Brusselmans M, et al. Diagnostic accuracy of ultrasound and MR imaging in peroneal neuropathy: A prospective, single-center study. Muscle Nerve. 2024 Sep;70(3):360–370. doi: 10.1002/mus.28187.
7. Song B, Marathe A, Chi B, Jayaram P. Hydrodissection as a therapeutic and diagnostic modality in treating peroneal nerve compression. Proc (Bayl Univ Med Cent). 2020 May 5;33(3):465–466. doi: 10.1080/08998280.2020.1758006.
8. Lam KHS, Hung CY, Chiang YP, Onishi K, Su DCJ, Clark TB, Reeves KD. Ultrasound-guided nerve hydrodissection for pain management: rationale, methods, current literature, and theoretical mechanisms. J Pain Res. 2020 Aug 4;13:1957–1968. doi: 10.2147/JPR.S247208.
9. Hildebrand G, Tompkins M, Macalena J. Fibular head as a landmark for identification of the common peroneal nerve: a cadaveric study. Arthroscopy. 2015 Jan;31(1):99–103. doi: 10.1016/j.arthro.2014.07.014.
10. Desy NM, Lipinski LJ, Tanaka S, Amrami KK, Rock MG, Spinner RJ. Recurrent intraneural ganglion cysts: Pathoanatomic patterns and treatment implications. Clin Anat. 2015 Nov;28(8):1058–1069. doi: 10.1002/ca.22615.
11. Kim JY, Song S, Park HJ, Rhee WI, Won SJ. Diagnostic cutoff value for ultrasonography of the common fibular neuropathy at the fibular head. Ann Rehabil Med. 2016 Dec;40(6):1057–1063. doi: 10.5535/arm.2016.40.6.1057.
12. Bignotti B, Assini A, Signori A, Martinoli C, Tagliafico A. Ultrasound versus MRI in common fibular neuropathy. Muscle Nerve. 2017 Jun;55(6):849–857. doi: 10.1002/mus.25418.
13. Tagliero LE, Strother CRC, Spinner RJ, Bishop AT, Shin AY. Accuracy of ultrasound and MRI in the diagnosis of common peroneal nerve injuries. Acta Neurochir (Wien). 2025 May 1;167(1):127. doi: 10.1007/s00701-025-06542-3.